DISCRIMINATING SILT-AND-CLAY FROM SUSPENDED-SAND IN RIVERS USING SIDE-LOOKING ACOUSTIC PROFILERS

Scott A. Wright, research hydrologist, USGS, Sacramento, CA, sawright@usgs.gov; David J. Topping, research hydrologist, USGS, Flagstaff, AZ, dtopping@usgs.gov; Cory A Williams, hydrologist, USGS, Grand Junction, CO, cawillia@usgs.gov

INTRODUCTION

The ability to accurately monitor suspended-sediment flux in rivers is needed to support many types of studies, because the sediment that typically travels in suspension affects geomorphology and aquatic habitat in a variety of ways (e.g. bank and floodplain deposition, bar morphology, light penetration and primary productivity, tidal wetland deposition in the context of sea-level rise, sediment-associated contaminants, reservoir sedimentation and potential erosion during dam removal, among others). In addition, human-induced changes to the landscape have resulted in substantially altered suspended-sediment loads (Syvitski et al., 2005). Thus, accurate monitoring of suspended-sediment flux is necessary for informed resource management of rivers.

Because of this need, a variety of techniques have been developed and applied for suspended-sediment monitoring. The traditional approach in the United States, which was developed and has been used extensively by the U.S. Geological Survey (USGS), is to collect an isokinetic, velocity-weighted sample from a river cross-section, analyze the sample in the laboratory, and use water-discharge records to compute a record of suspended-sediment flux (Guy, 1969, Guy, 1970, Edwards and Glysson, 1999, Porterfield, 1972). The labor and expense associated with this traditional approach is substantial such that the number of USGS gages reporting daily records of suspended-sediment flux decreased from 364 in 1981 to 120 in 2003 (Osterkamp et al., 2004). Also, the traditional sampling approach is limited with respect to the temporal resolution that can be achieved, thus requiring the use of approximate relations between suspended-sediment concentration and water discharge to fill gaps between samples. To address these limitations, several indirect or "surrogate" measures have been investigated (see e.g. Gray and Gartner, 2009) most notably optical backscatter (i.e. turbidity), laser-diffraction, and acoustic backscatter. These indirect techniques rely on measurements of ancillary properties that correlate with suspended-sediment concentration and particle size and thus require the collection of traditional samples for calibration. Through *in situ* deployments, these methods can provide the high temporal resolution that cannot be achieved through traditional sampling.

Here we focus on the evaluation of acoustic profiling techniques (e.g. acoustic-Doppler sideways-looking profilers, or ADPs). One major advantage of acoustic profiling is the ability to concurrently measure water velocity (using Doppler-shift methods) and suspended-sediment concentration such that suspended-sediment flux can be directly computed using data from a single instrument. Acoustic-Doppler profilers have become popular for measuring water velocity and discharge in rivers, through both moving-boat operations and from fixed deployments such as bank-mounted sideways-looking instruments (Hirsch and Costa, 2004, Muste et al., 2007). The method presented herein is most suited to sideways-looking applications as a complement to the "index velocity" technique, whereby an index velocity from a sideways-looking instrument is related to the cross-section average velocity (determined from moving-boat discharge

measurements) as a means for developing a continuous water-discharge record (Ruhl and Simpson, 2005).

Topping et al. (2007) presented a method for discriminating silt-and-clay from suspended sand, using single frequency ADPs. This method takes advantage of the relations among acoustic backscatter, sediment-induced acoustic attenuation, suspended-sediment concentration (SSC), and particle size distribution (PSD). Backscatter is the amount of sound scattered back and received at the transducer while sediment-induced attenuation is the amount of sound scattered in other directions and absorbed by the sediment particles. Both of these parameters can be measured with an ADP, and their different dependencies on SSC and PSD allow for the discrimination of suspended silt-and-clay from suspended sand. Topping et al. (2007) describe application of the method at several sites along the Colorado River in Grand Canyon, and herein we present an example application of the technique for the Gunnison River, CO. However, the methods' general applicability in rivers has yet to be evaluated due to a lack of concurrent acoustic and sediment data at a range of sites. To this end, the objective of the analysis presented herein is to evaluate the potential general applicability of the method, drawing from the extensive USGS database on SSC and PSD. We refer to it as "potential" general applicability because it relies on the theory underlying the previous empirical results. Use of the theoretical relations is necessary due to the lack of concurrent ADP and SSC/PSD data, but also serves the additional purpose of providing further justification of the empirical calibrations developed for the Colorado and Gunnison Rivers.

METHOD FOR DISCRIMINATING SILT-AND-CLAY FROM SUSPENDED SAND

The equations governing the scattering of sound by small particles (e.g. silt and sand sizes) at megahertz frequencies (e.g. 0.5 – 5 MHz), as well as their application for a variety of purposes under a range of environmental conditions (primarily coastal applications), were published in a series of papers in the late 1980s and 1990s (e.g. Hanes et al., 1988, Sheng and Hay, 1988, Hay, 1991, Thorne et al., 1991, Hay and Sheng, 1992, Thorne and Campbell, 1992, Crawford and Hay, 1993, Thorne et al., 1993, Thorne et al., 1995, Richards et al., 1996, Thorne and Hardcastle, 1996, Schaafsma and Hay, 1997, Thorne and Hardcastle, 1997, among others). A comprehensive review of the techniques and applications was conducted by Thorne and Hanes (2002). Herein we focus on describing and testing the method of Topping et al. (2007) for discriminating silt-and-clay from suspended sand.

The starting point for the method is the theoretical relation between SSC and backscatter (e.g. Gartner, 2004, Thorne and Hanes, 2002):

$$\log_{10}\{SSC\} = 0.1(RL + 2TL) + K_T \quad (1)$$

where RL is the reverberation (or backscatter) level, TL denotes transmission losses that occur along the acoustic beam, K_T is an instrument- and site-specific constant (also dependent on particle size), and 0.1 is the theoretical value of the slope (though practical experience indicates that the slope is instrument- and site-specific as well). Note that eq. 1 can be derived from the equations presented in Thorne and Hanes (2002), which are written in terms of pressure and intensity, by conversion to decibel units using base 10 log transformations. ADPs measure the

reverberation level and report it either as a signal-to-noise ratio (SNR, in dB) or as a raw signal strength (in counts, which are proportional to dB, e.g. Gartner, 2004). The term (*RL* + *2TL*) represents the "adjusted" backscatter, i.e. the backscatter recorded by the instrument corrected for the transmission losses occurring along the beam path (described below). Linear regression can thus be used to determine the slope and y-intercept (K_T) of the relation given concurrent measurements of *SSC* and *RL*, so long as *TL* can be estimated. Though the theoretical value of the slope is known, it is typically considered unknown and estimated from regression (providing a further test of the theory). Transmission losses along the beam result from beam spreading, sound absorption by the fluid, and sound attenuation by the sediment (e.g. Gartner, 2004):

$$2TL = 20\log_{10} r + 2\alpha_f r + 2\alpha_s r \tag{2}$$

where α_f and α_s are fluid-absorption and sediment-attenuation coefficients (in dB/m), respectively, and *r* is range from the instrument along the beam.

The calculations necessary for discriminating silt-and-clay from suspended sand proceed in three steps. The first step is to correct the measured backscatter (*RL*) for losses not related to sediment properties, i.e. beam spreading and fluid absorption. This results in a "fluid-corrected backscatter" profile, *FCB*:

$$FCB = RL + 20\log_{10} r + 2\alpha_f r \tag{3}$$

As an example, figure 1 shows the measured backscatter (*RL*) and fluid-corrected backscatter (*FCB*) for a single profile measurement from the Gunnison River, CO (USGS gage 09152500, 1,500 kHz side-looking instrument, 1-m blank, 10 cells, 1-m cell size, 25° beam angle, α_f from Schulkin and Marsh, 1962).

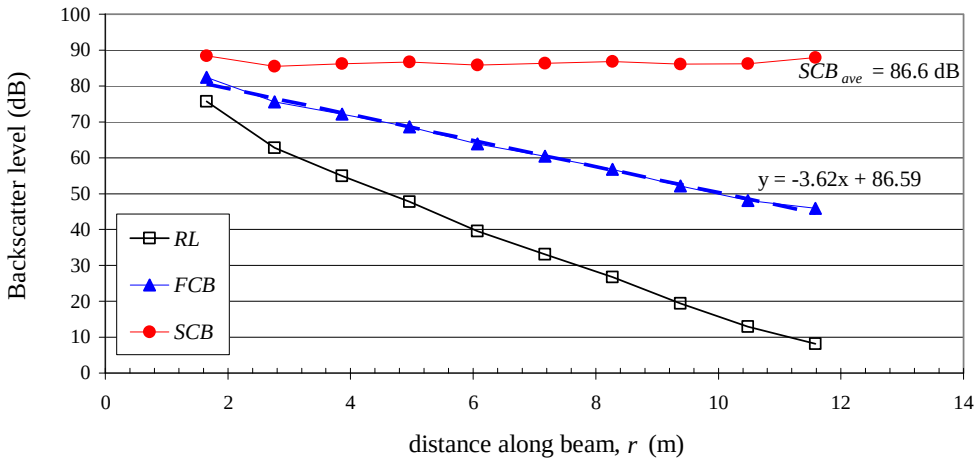

Figure 1 Example of measured and corrected backscatter profiles from the Gunnison River, CO.

Next, the sediment attenuation coefficient is estimated from the *FCB* profile by assuming that the lateral distribution in sediment concentration and particle size is roughly uniform. Under this assumption, the slope of the *FCB* profile represents attenuation losses due to the sediment:

$$\alpha_s = -\frac{1}{2}\overline{\frac{d}{dr}(FCB)} \tag{4}$$

where the $-1/2$ multiplier accounts for the fact that losses occur in both directions along the beam. For the Gunnison River example in figure 1, the slope of the *FCB* profile is -3.62, yielding $\alpha_s = 1.81$ dB/m. Once the sediment attenuation coefficient has been computed, these losses can be removed from the FCB profile yielding the "sediment-corrected backscatter", *SCB*:

$$SCB = FCB + 2\alpha_s r \tag{5}$$

The *SCB* profile for the Gunnison River example is shown in figure 1, and represents the backscatter level along the beam with all of the losses removed. The *SCB* profile can then be averaged along the beam to yield a bulk backscatter level; for the example in figure 1 this yields SCB_{ave} = 86.6 dB. The sediment-attenuation coefficient (α_s) and the bulk-sediment-corrected backscatter (SCB_{ave}) are the two measured parameters that provide the basis for discriminating silt-and-clay from suspended sand, as described below.

Topping et al. (2007) showed that for the Colorado River in Grand Canyon, using the same methods described here, the sediment-attenuation coefficient tended to correlate strongly with silt-and-clay concentrations, whereas the backscatter level correlated with suspended-sand concentration. The Gunnison River data also display these correlations as shown in figure 2. The attenuation calibration (left panel) exhibits the expected linear dependence (next section) and the backscatter calibration (right panel) yielded a fitted slope of 0.13, which is close to the theoretical value of 0.1 (eq. 1). This example provides further empirical support for the technique. The theoretical underpinnings are detailed in the next section along with application of the theory to a large dataset from rivers in the U.S. The Gunnison River sediment data are described in detail in Williams et al. (2009).

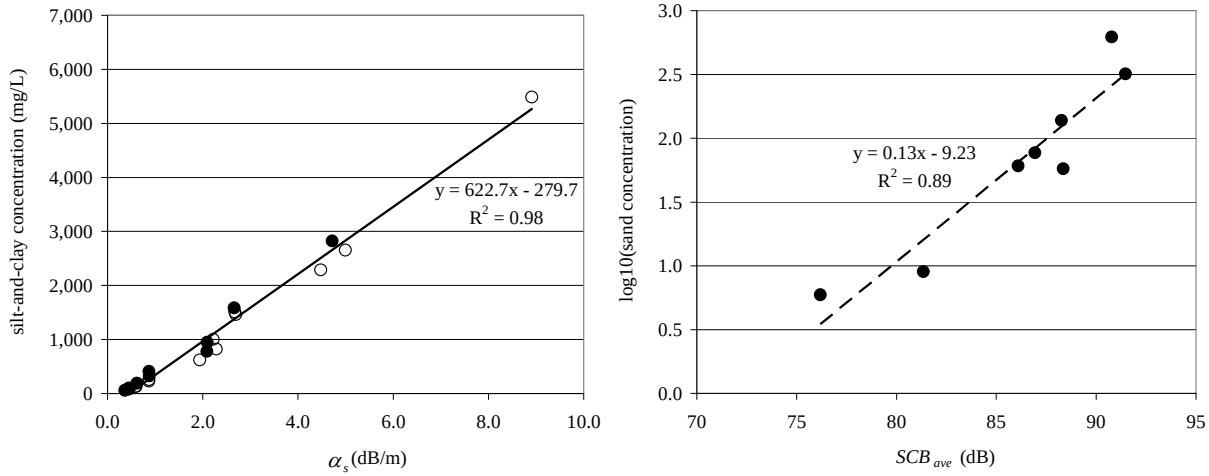

Figure 2 Silt-and-clay concentration versus sediment attenuation (left) and suspended-sand concentration versus backscatter (right) for the Gunnison River, CO.

THEORETICAL SUPPORT FOR THE METHOD

To understand why attenuation tends to correlate with silt-and-clay, whereas backscatter tends to correlate well with suspended sand, it is necessary to examine the relations among attenuation, backscatter, sediment concentration, and particle size. For backscatter, the relative level (above a source level that is instrument specific) depends primarily on the SSC and PSD of the suspension. In terms of intensity (square of pressure), the relation among backscatter, concentration, and particle size is as follows (see e.g. Thorne and Hanes, 2002, eq. 7):

$$\frac{BS}{SSC} \propto \frac{f^2}{D} \tag{6}$$

where *BS* denotes relative backscatter intensity, *D* is particle diameter, and *f* is a "form function" describing the scattering properties of the sediment (for a given acoustic frequency). The form function has been estimated experimentally by several researchers and, for the typical ADP frequencies deployed and suspended-sediment particle sizes in rivers, the general relation is $f \propto D^2$. Thus, backscatter is expected to increase as approximately the cube of particle size, for a given suspended-sediment concentration.

The relations between attenuation, concentration, and particle size are slightly more complex than the backscatter relations, but these relations have been derived and tested by several researchers. For example, Urick (1948) provides the theoretical relation (eq. 5 therein) and Flammer (1962) provides a summary of the physical mechanisms leading to attenuation losses. More recent work has refined the relation in the scattering-loss range (e.g. Thorne and Hanes, 2002, fig. 3b therein). The detailed equations are not presented here due to space limiations; however, figure 3 shows the relations in graphical form for both backscatter and attenuation, each scaled by *SSC*, as functions of particle size.

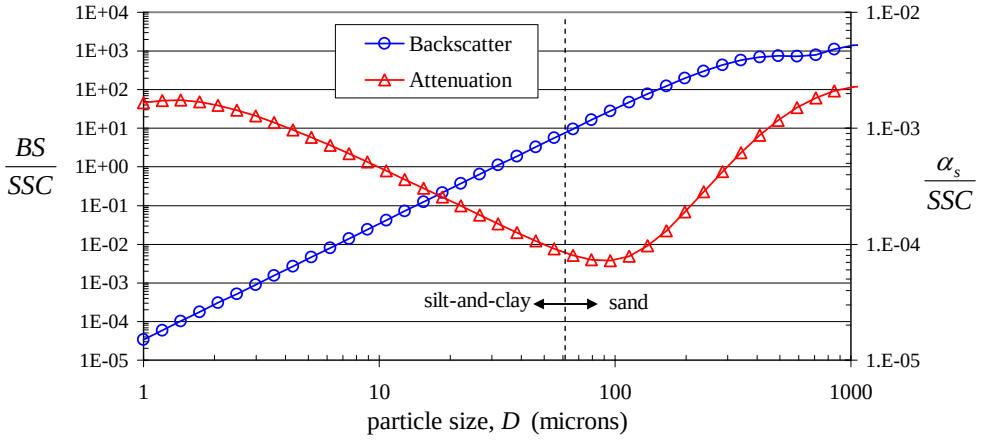

Figure 3 Theoretical relations for backscatter (left axis, blue) and attenuation (right axis, red), for a given suspended-sediment concentration, as a function of particle size (at 1 MHz frequency).

In figure 3, eq. 6 was used to compute *BS/SSC* with *f* computed from Thorne and Hanes (2002, eq. 10a therein), α_s was computed from Urick (1948, eq. 5 therein) for the viscous component

and Thorne and Hanes (2002, eqs. 8, 9, and 10b therein) for the scattering component. Figure 3 provides the theoretical basis for the method, as it is seen that attenuation and backscatter trend in different directions with particle size for typical ADP frequencies and for particle sizes typically in suspension in rivers (i.e. <250 μm). Attenuation is highest for the finest particle sizes – the same concentration of clay attenuates an order of magnitude more acoustic energy than fine sand. Scattering-loss attenuation becomes high for coarse sand but these particle sizes are not typically in suspension in rivers. Conversely, backscatter increases monotonically with particle size such that sand backscatters orders of magnitude more sound than clay. Thus, for a uniform particle-size distribution, clay sizes would tend to dominate attenuation while sand sizes would dominate backscatter. It is noted that the relations in figure 3 are for 1 MHz frequency; decreasing frequency shifts the attenuation curve down and to the right (i.e. less attenuation for a given particle size) and shifts the backscatter curve downward. However, for the range of typical ADP frequencies (e.g. 0.5 – 3 MHz), the basic structure of the relations remains similar.

APPLICATION OF THE THEORY TO DATA FROM A RANGE OF RIVERS

Further empirical testing of the method requires additional concurrent ADP and sediment-concentration and particle-size data for a variety of river conditions. However, because the underlying theory strongly supports the empirical findings, it's constructive to evaluate the method in the context of available historical suspended-sediment data. To this end, we applied the equations underlying figure 3 (references provided in the previous section) to suspended-sediment concentration and particle-size measurements from a large dataset of U.S. rivers (described below). We have assumed that the theory can be applied to narrow particle-size ranges (1-φ increments) and summed to compute the total backscatter and attenuation. Application of the theoretical relations yields probability density functions (PDFs) for *SSC*, attenuation, and backscatter, as follows:

$$p(SSC_i) = SSC_i \Big/ \sum_{i=1}^{N} SSC_i \tag{7}$$

$$p(\alpha_{si}) = \alpha_{si} \Big/ \sum_{i=1}^{N} \alpha_{si} \tag{8}$$

$$p(BS_i) = BS_i \Big/ \sum_{i=1}^{N} BS_i \tag{9}$$

where *i* denotes the individual particle-size range and *N* is the total number of particle-size ranges. The PDFs were used to compute the fraction of the total attenuation attributable to silt-and-clay ($F_{\alpha-sc}$) and the fraction of the total backscatter attributable to suspended sand ($F_{\beta-sand}$), as follows:

$$F_{\alpha_s-sc} = \sum_{sc} p(\alpha_{si}) \tag{10}$$

$$F_{BS-sand} = \sum_{sand} p(BS_i) \tag{11}$$

where "sc" and "sand" denote summations over the silt-and-clay and sand particle-size ranges, respectively (finer than 62 μm and from 62 – 2,000 μm). By definition, the PDFs sum to unity

over all particle-size ranges; thus, for the method to have general applicability $F_{\alpha_s - sc}$ and $F_{BS-sand}$ should both tend toward unity over a range of conditions, indicating that attenuation is mostly caused by silt-and-clay sizes while backscatter is mostly caused by sand sizes.

We compiled a suspended-sediment dataset based on the 1990 summary of the largest rivers in the U.S. (Kammerer, 1990). This compilation includes all rivers in the top 20 in discharge, drainage area, or length, resulting in a total of 32 rivers spanning a broad range of hydrologic and geologic settings. Suspended-sediment concentration and particle-size data were obtained from the USGS water-quality database (http://nwis.waterdata.usgs.gov/usa/nwis/qwdata); the procedures used for collection and analysis of these data are described in Edwards and Glysson (1999) and Guy (1969). Suspended-sediment data were available for 21 of the rivers, with the number of samples for each ranging from 7 to 277. Table 1 below summarizes the river dataset.

Table 1 Summary of river data used in this study.

River	Date range	# of samples	*SSC* range (mg/L)	Range in % silt-and-clay	USGS gage #
Arkansas	Jun-48 – Sep-81	15	200 – 5,900	73 - 98	07152500, 07164500
Brazos	Feb-66 – Jun-86	119	15 – 9,440	59 - 100	08114000
Canadian	May-49 – Jul-50	16	135 – 141,000	60 - 100	07227500, 07228500
Colorado (TX)	Dec-69 – Apr-73	16	278 – 3,630	83 - 100	08161000
Copper	Aug-54 – Sep-86	39	183 – 3,900	53 - 82	15212000
Gila	Aug-60 – Mar-86	95	175 – 200,000	40 -100	09474000
Kansas	Jun-48 – Aug-50	97	270 – 33,000	56 - 100	06892500
Kuskokwim	Jun-66 – Sep-86	15	93 – 880	43 - 87	15304000
Mississippi	Apr-60 – Jun-73	41	143 – 2,080	52 - 96	07010000
Missouri	Mar-73 – Feb-76	16	676 – 2,390	53 - 87	06807000, 06610000
Ohio	Nov-79 – Jun-82	24	261 – 908	72 - 98	03294500
Pecos	Oct-60 – May-89	277	55 – 20,300	62 - 100	08396500
Platte	Mar-73 – Jun-93	37	561 – 14,100	39 - 99	06805500
Red	Nov-79 – Jun-81	7	1,070 – 8,720	38 - 98	07316000
Rio Grande	Apr-66 – Feb-83	62	366 – 7,000	69 - 100	08475000
Sacramento	Feb-58 – Mar-80	98	20 – 1,970	35 - 98	11447500
San Joaquin	Jul-67 – Sep-89	85	42 – 424	54 - 100	11303500
Stikine	Jun-76 – Jul-86	26	144 – 1,290	34 - 81	15024800
Susitna	Jul-75 – Jul-86	14	257 – 1,490	41 - 81	15294350
Susquehanna	Aug-79 – Feb-84	23	17 – 359	97 - 100	01578310
Tanana	May-66 – Jun-83	19	411 – 2,680	16 - 89	15515500
Yellowstone	Apr-83 – Jun-91	21	173 – 8,770	67 - 100	06329500
Yukon	Jun-75 – Sep-86	13	141 – 997	59 - 93	15565447

RESULTS AND DISCUSSION

Application of eqs. 7-9 to the concentration and particle-size data from all of the rivers in table 1 yields the box-and-whisker PDFs shown in figure 4.

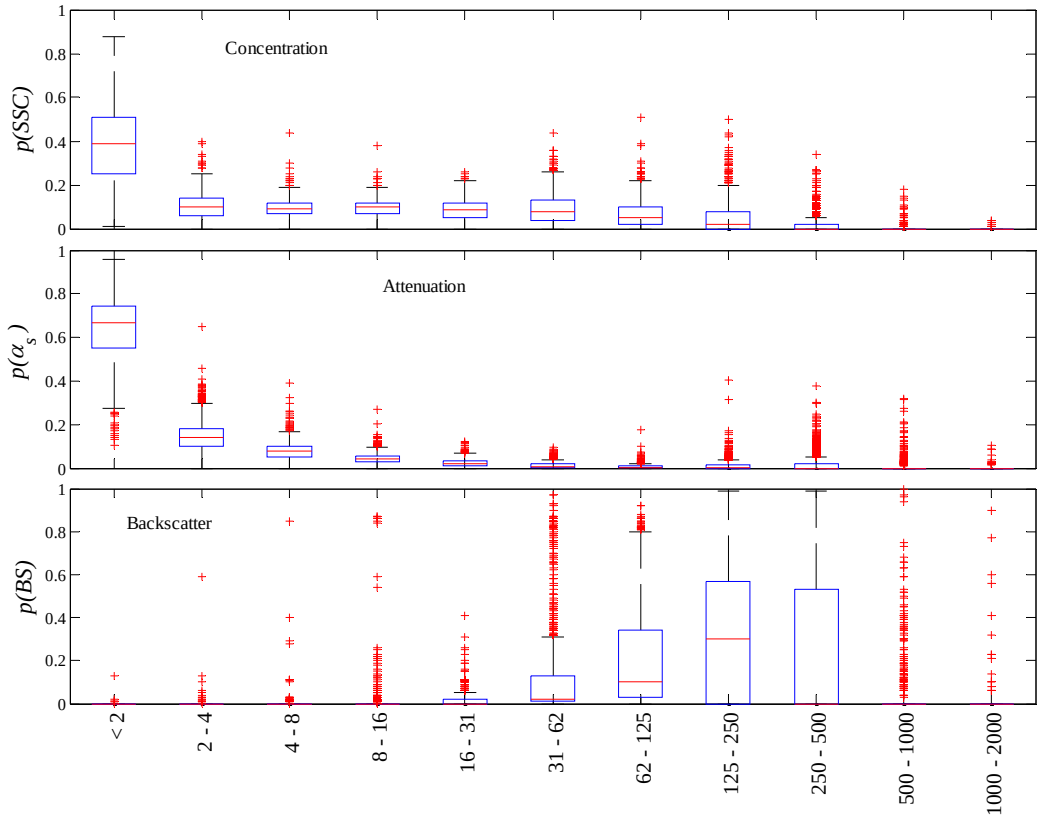

Figure 4 PDFs of concentration (top), attenuation (middle), and backscatter (bottom) for river data used in this study (see Table 1). X-axis particle-size ranges are in microns. Red lines denote median values, box extents are 25th and 75th percentiles, whiskers lengths are 1.5 times the interquartile range, and points outside this range are red pluses.

From the *SSC* PDF (top) it is apparent that suspended sediment tends to be dominated by the finest size range (<2 μm). It is noted that particle-size analyses were performed on the primary particles, i.e. after taking measures to de-flocculate the sediment (Guy, 1969). For sizes greater than 2 μm, there is a general trend of decreasing fractional representation with increasing size with very little representation of sizes greater than 250 μm.

The prevalence of the finest sizes in the *SSC* PDFs results in these sizes dominating the attenuation as well (figure 4, middle). This is explained by examining figure 3 (right axis, red triangles) which shows that attenuation is strongly inversely proportion to particle size such that clay attenuates much more sound than fine sand (for an equivalent concentration). The results shown in figure 4 were obtained using an acoustic frequency of 1,000 kHz, but similar results (not shown) were obtained using 500 and 2,000 kHz frequencies as well.

The backscatter results (figure 4, bottom) exhibit the opposite trend as attenuation, such that the sand sizes tend to dominate despite their relatively small representation in the *SSC* PDFs. The reason for this is again apparent from figure 3 (left axis, blue circles) which shows that backscatter is strongly directly proportional to particle size; thus, sand backscatters substantially more sound than clay. It follows that even though there is typically less sand in suspension than silt-and-clay, its larger particle size leads to proportionally more backscatter. The fractional peak in backscatter tends to occur in the fine-sand particle-size range (125 – 250 μm) because it tends to be the largest particle size that is suspended in appreciable amounts in the rivers studied.

The PDFs in figure 4 were summed over the silt-and-clay and sand particle-size ranges, through application of eqs. 10-11. This yields the fraction of attenuation and backscatter due to these particle-size ranges, respectively, and the results are shown in figure 5.

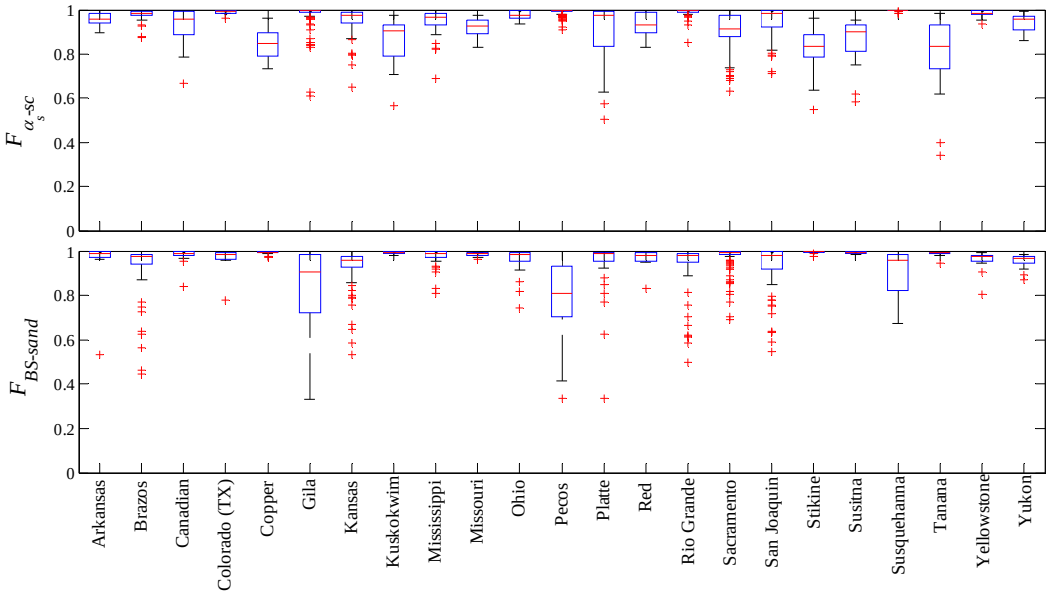

Figure 5 Computed fraction of attenuation due to silt-and-clay (top) and fraction of backscatter due to sand (bottom) for all samples from each river (see table 1).

Figure 5 indicates that $F_{\alpha_s - sc}$ and $F_{BS-sand}$ both tend toward unity for all of the rivers in the dataset, with median values all greater than 80% and all lower quartiles exceeding 70%. Though there are a few samples for most rivers with fractions approaching or below 50%, there is a general trend for silt-and-clay to dominate attenuation and for sand to dominate backscatter. Thus, figure 5 provides strong evidence that the method for discriminating silt-and-clay from suspended sand, as outlined theoretically and demonstrated herein for the Gunnison River, should have some general applicability over a wide range of conditions encountered in most rivers.

One limitation of the calculations is that the measured PSDs are based on laboratory analyses of the primary particles, i.e. after de-flocculation, and thus likely do not perfectly represent the *in situ* PSDs. Flocculation is a common phenomenon in estuaries and has also been documented in rivers, for example below wastewater treatment plants (Krishnappan, 2000). A few of the rivers

in the dataset contained analyzes of PSDs in their native water and these size distributions allow for a rough evaluation of the effects of flocculation. For these samples, the native water particle-size distributions show that the finest sizes tend to flocculate almost exclusively into the 8-16 µm size range. Thus, though this would affect the total amount of computed attenuation, it likely would not affect the conclusion that silt-and-clay dominates attenuation. Also, this flocculation would tend to increase backscatter due to silt-and-clay, but the highly non-linear nature of the size-backscatter relation (figure 2, left axis, blue circles) suggests that sand sizes would still dominate backscatter. However, the only definitive method for evaluating this effect is the collection of *in situ* particle-size distribution data (e.g. with laser-diffraction instruments) at the particular river cross-section where acoustic and suspended-sediment data are being collected.

CONCLUSIONS

This study describes and further tests the method for discriminating silt-and-clay from suspended sand in rivers using sideways-looking ADPs, as first outlined and applied by Topping et al. (2007). The discrimination is possible due to the forms of the relations between suspended-sediment concentration, particle size, sediment-induced attenuation, and backscatter. The method was demonstrated empirically herein through an example application on the Gunnison River, CO, which supplements previous applications on the Colorado River in Grand Canyon (Topping et al., 2007). The empirical success of the method was then explained within the theoretical framework governing sound backscatter and attenuation by suspended particles in water at megahertz frequencies. To test the potential general applicability of the method, we assembled concentration and particle-size data from a wide range of river settings throughout the U.S., and applied the theoretical relations underlying the method to this dataset. The results confirm the empirical findings on the Gunnison and Colorado Rivers, i.e. that attenuation tends to be dominated by the silt-and-clay particle-size fraction while backscatter tends to be dominated by the sand particle-size fraction. Because sideways-looking ADPs can measure both attenuation and backscatter, the relative fractions of silt-and-clay versus sand in suspension can be determined. For the 23 rivers examined in this study, the fraction of attenuation attributable to silt-and-clay had median values greater than 80%; similar results were obtained for the fraction of backscatter attributable to sand. Thus, we believe that the method is likely to have general applicability for a wide range of river conditions. The primary limitation of the method, as with any single-frequency application, is that large changes in the particle-size distributions in suspension will tend to shift the calibrations. Thus, a multi-frequency approach (as described in Topping et al, 2007) that employs the same techniques may be necessary for some rivers, and this can only be evaluated on a site-to-site basis.

The findings from this study add to the reasons why ADPs are gaining popularity in river monitoring. From a sediment monitoring perspective, ADPs have distinct advantages over other methods, such as traditional “bottle” sampling and optical techniques (e.g. turbidity monitoring). ADPs can be deployed *in situ* thus providing high temporal resolution (e.g. 15 minutes, which is the standard for stage and discharge records). Profiling capabilities allow ADPs to “sample” very large volumes of water, potentially spanning the entire width of the river cross-section. In our experience, acoustic instruments are less prone to biological fouling than optical instruments, though fouling can occur with ADPs as well. Finally, many gaging stations are already equipped with sideways-looking ADPs to measure “index” velocity and stage for flow monitoring. The results of our study suggest that these ADPs, once calibrated based on episodic sediment

measurements, could provide concurrent records of silt-and-clay and suspended-sand flux, at relatively low additional cost.

REFERENCES

Crawford, A.M. and Hay, A.E. (1993). "Determining suspended sand size and concentration from multifrequency acoustic backscatter", J. Acoust. Soc. Am. 94(6), pp 3312-3324.

Edwards, T.K., and Glysson, G.D. (1999). "Field Methods for Measurement of Fluvial Sediment", U.S. Geological Survey Techniques of Water-Resources Investigations, Book 3, Chapter C2, 89 pp., http://pubs.usgs.gov/twri/twri3-c2/pdf/TWRI_3-C2.pdf

Flammer, G.H. (1962). "Ultrasonic measurement of suspended sediment", U.S. Geological Survey Bulletin 1141-A. Government Printing Office, Washington, DC, 48 pp.

Gartner, J. W. (2004). "Estimating suspended solids concentrations from backscatter intensity measured by acoustic Doppler current profiler in San Francisco Bay, California", Mar. Geol., 211, pp 169-187.

Gray, J. R., and J. W. Gartner (2009). "Technological advances in suspended-sediment surrogate monitoring", Water Resour. Res., 45, W00D29, doi:10.1029/2008WR007063.

Guy, H.P. (1969). "Laboratory Theory and Methods for Sediment Analysis", U.S. Geological Survey, Techniques of Water-Resources Investigations, Book 5, Chapter C1, 59 pp., http://pubs.usgs.gov/twri/twri5c1/pdf/TWRI_5-C1.pdf

Guy, H.P. (1970). "Fluvial Sediment Concepts", *U.S. Geological Survey, Techniques of Water-Resources Investigations, Book 3, Chapter C1*, 55 pp., http://pubs.usgs.gov/twri/twri3-c1/pdf/TWRI_3-C1.pdf

Hanes, D. M., Vincent, C. E., Huntley, D. A., and Clarke, T. L. (1988). "Acoustic measurements of suspended sand concentration in the C2S2 experiment at Stanhope Lane, Prince Edward Island", Mar. Geol., 81, pp 185-196.

Hay, A. E. (1991). "Sound scattering from a particle-laden, turbulent jet", J. Acoust. Soc. Am., 90(4) pt. 1, pp 2055-2074.

Hay, A. E. and Sheng, J. (1992). "Vertical profiles of suspended sand concentration and size from multi-frequency acoustic backscatter", J. of Geo. Res., 97(C10), pp 15661-15677.

Hirsch, R.M., and Costa, J.E. (2004). "U.S. stream flow measurement and data dissemination improve", Eos Trans. AGU, 85(20), p 197, p 203.

Kammerer, J.C. (1990). "Largest Rivers in the United States", U.S. Geological Survey Water Fact Sheet, Open-File Report 87-242, 2 pp.

Krishnappan, B.G. (2000). "In situ size distribution of suspended particles in the Fraser River", J. Hyd. Eng., 126(8), pp 561-569.

Muste, M., Vermeyen, T., Hotchkiss, R., and Oberg, K. (2007). "Acoustic Velocimetry for Riverine Environments", J. Hydr. Engrg., 133(12), pp 1297-1298.

Osterkamp, W.R., Heilman, P., and Gray, J.R. (2004). "An Invitation to Participate in a North American Sediment-Monitoring Network", Eos, Trans. AGU, 85(40), doi:10.1029/2004EO400005

Porterfield, G. (1972). "Computation of Fluvial-Sediment Discharge", U.S. Geological Survey, Techniques of Water-Resources Investigations, Book 3, Chapter C3, 66 pp., http://pubs.usgs.gov/twri/twri3-c3/pdf/TWRI_3-C3.pdf

Richards, S.D., Heathershaw, A.D., and Thorne, P.D. (1996). "The effect of suspended particulate matter on sound attenuation in seawater", J. Acoust. Soc. Am., 100(3), pp 1447-1450.

Ruhl, C.A., and Simpson, M.R. (2005). “Computation of Discharge Using the Index-Velocity Method in Tidally Affected Areas”, U.S. Geological Survey Scientific Investigations Report 2005-5004, http://pubs.usgs.gov/sir/2005/5004/sir20055004.pdf

Schaafsma, A.S. and Hay, A.E. (1997). “Attenuation in suspensions of irregularly shaped sediment particles: A two-parameter equivalent spherical scatterer model”, J. Acoust. Soc. Am., 102(3), pp 1485-1502.

Schulkin, M., and Marsh, H.W. (1962). “Sound absorption in sea water”, J. Acoust. Soc. Am., 34(6), pp 864-865.

Sheng, J. and Hay, A.E. (1988). “An examination of the spherical scatter approximation in aqueous suspensions of sand”, J. Acoust. Soc. Am., 83(2), pp 598-610.

Syvitski, J.P.M., Vorosmarty, C.J., Kettner, A.J., and Green, P. (2005). “Impact of Humans on the Flux of Terrestrial Sediment to the Global Coastal Ocean”, Science, 308, pp 376-380.

Thorne, P.D., Vincent, C.E., Harcastle, P.J., Rehman, S., and Pearson, N. (1991). “Measuring suspended sediment concentrations using acoustic backscatter devices”, Mar. Geol., 98, pp 7-16.

Thorne, P.D. and Campbell, S.C. (1992). “Backscattering by a suspension of spheres”, J. Acoust. Soc. Am., 92(2), pp 978-986.

Thorne, P.D., Hardcastle, P.J., and Souslby, R.L. (1993). “Analysis of acoustic measurements of suspended sediment”, J. Geophys. Res., 98(C1), pp 899-910.

Thorne, P.D., Waters, K.R., and Brudner, T.J. (1995). “Acoustic measurements of scattering by objects of irregular shape”, J. Acoust. Soc. Am., 97(1), pp 242-251.

Thorne, P.D., Hardcastle, P.J., and Hogg, A. (1996). “Observations of near-bed suspended sediment turbulence structures using multifrequency acoustic backscatter”, in Coherent Flow Structures in Open Channels, eds. P.J. Ashworth, S.J. Bennet, J.L. Best and S.J. McLelland, John Wiley & Sons Ltd.

Thorne, P.D. and Hardcastle, P.J. (1997). “Acoustic measurement of suspended sediments in turbulent currents and comparison with in-situ samples”, J. Acoust. Soc. Am., 101(5), pp 2603-2614.

Thorne, P.D., and Hanes, D.M. (2002). “A review of acoustic measurements of small-scale sediment processes”, Cont. Shelf Res., 22, pp 603-632.

Topping, D.J., Wright, S.A., Melis, T.S., and Rubin, D.M. (2007). “High-resolution measurements of suspended-sediment concentration and grain size in the Colorado River in Grand Canyon using a multi-frequency acoustic system”, in Proceedings of the 10th International Symposium on River Sedimentation. August 1–4, Moscow, Russia.

Urick, R.J. (1948). “The absorption of sound in suspensions of irregular particles”, J. Acoust. Soc. Am., 20(3), pp 283-289.

Williams, C.A., Gerner, S.J., and Elliott, J.G. (2009). “Summary of fluvial sediment collected at selected sites on the Gunnison River in Colorado and the Green and Duchesne Rivers in Utah, water years 2005–2008”, U.S. Geological Survey Data Series 409, 123 pp.